Piecewise-linear soliton equations and piecewise-linear integrable maps

2001 J. Phys. A: Math. Gen. 34 2491

(http://iopscience.iop.org/0305-4470/34/11/337)

INSTITUTE OF PHYSICS PUBLISHING JOURNAL OF PHYSICS A: MATHEMATICAL AND GENERAL

J. Phys. A: Math. Gen. **34** (2001) 2491–2503 www.iop.org/Journals/ja PII: S0305-4470(01)14700-1

Piecewise-linear soliton equations and piecewise-linear integrable maps

G R W Quispel[1], **H W Capel**[2] **and J Scully**[1]

[1] Department of Mathematics, La Trobe University, Bundoora, Melbourne, 3083, Australia
[2] Institute of Theoretical Physics, University of Amsterdam, Valckenierstraat 65, 1018 XE Amsterdam, The Netherlands

E-mail: R.Quispel@latrobe.edu.au

Received 14 June 2000, in final form 4 January 2001

Abstract
We study piecewise-linear integrable systems. The associated piecewise-linear solitons, piecewise-linear integrable maps and piecewise-linear Lax representation are discussed.

PACS numbers: 0230I, 0545Y, 4520J

(Some figures in this article are in colour only in the electronic version; see www.iop.org)

1. Introduction

Integrable dynamical systems have a long and distinguished history. The oldest are differential equations. Famous examples in finite dimensions include the Kepler problem [3], various spinning tops [4] and the (continuous) Painlevé equations [1]. In infinite dimensions one gets soliton equations [6]. Some well known examples are the Korteweg–de Vries equation, the sine-Gordon equation and the nonlinear Schrödinger equation.

More recently, various integrable discrete analogues have been studied: integrable (partial) difference equations [2, 9, 16], integrable maps [5, 13, 15, 17, 18, 24], discrete Painlevé equations [7] and integrable cellular automata [14, 22, 23].

In [23] a transformation combined with a limiting procedure was introduced to obtain new integrable equations (see also [22]). The ensuing novel integrable equations can be considered in various ways. In particular:

(i) The new transformed variables and parameters can be restricted to be integers. This case has received most attention to date.
(ii) The new transformed variables and parameters can be restricted to take any real values. This case, which was most notably studied in [8], is the case we will study in this paper. Through some examples we will discuss piecewise-linear solitons and piecewise-linear integrable maps.

As the analysis of case (i) is rather different from the analysis of case (ii), we will distinguish the two cases for the purposes of this paper by referring to systems (i) as 'ultradiscrete'[3], and by referring to systems (ii) as 'piecewise-linear'.

A similarity between ultradiscrete systems and piecewise-linear systems (as defined above) is that in both cases solitons are compact, a crucial aspect in physical applications. Differences between the two kinds of systems, and a further discussion of the physical relevance of piecewise-linear systems, are given in the concluding section of this paper.

2. Piecewise-linear kink solitons

2.1. Piecewise-linear equation and piecewise-linear one-kink solution

Consider the following integrable partial difference equation, the discrete modified Korteweg–de Vries (MKdV) equation [11]:

$$v(x, y+1) = v(x+1, y)\frac{v(x+1, y+1) + gtv(x, y)}{tv(x+1, y+1) + fv(x, y)} \tag{1}$$

with

$$f + t = 1 + gt. \tag{2}$$

Here the parameters f, g, t and the dependent variable v are assumed to be non-negative (and real), and the independent variables x and y are assumed to be *continuous* variables that can take on *any* real values (i.e. x, y, f, g, t and v are not discrete and *not* restricted to be integers).

It is well known that equation (1) is integrable and that it possesses n-kink solutions [11]. The Lax representation of the discrete MKdV equation (1) is given by

$$\underline{\boldsymbol{u}}(x+1, y) = \underline{\underline{l}}(x, y)\underline{\boldsymbol{u}}(x, y) \qquad \underline{\boldsymbol{u}}(x, y+1) = \underline{\underline{m}}(x, y)\underline{\boldsymbol{u}}(x, y) \tag{3}$$

where the Lax matrices $\underline{\underline{l}}$ and $\underline{\underline{m}}$ are given by

$$\begin{aligned} \underline{\underline{l}} &= \begin{pmatrix} f & tv(x+1, y) \\ tk/v(x, y) & v(x+1, y)/v(x, y) \end{pmatrix} \\ \underline{\underline{m}} &= \begin{pmatrix} g & v(x, y+1) \\ k/v(x, y) & v(x, y+1)/v(x, y) \end{pmatrix} \end{aligned} \tag{4}$$

where k is a spectral parameter and $\underline{\boldsymbol{u}}(x, y)$ is a two-dimensional vector (depending on k as well). Taking the compatibility condition of the two equations in (3), and substituting (4), we obtain the discrete MKdV equation (1).

The solutions of the discrete MKdV equation can be derived from a linear integral equation given in [11]. For example, the one-kink solution of equation (1) is given by

$$v(x, y) = \frac{1 + ca^x b^y s}{1 + ca^x b^y} \tag{5}$$

where c and s are arbitrary constants, and a, b and s are related by

$$\begin{aligned} a &= \frac{1 + fs}{f + s} \\ b &= \frac{1 + gs}{g + s}. \end{aligned} \tag{6}$$

[3] This name has been frequently used to refer to both cases (i) and (ii).

We now show how to take the piecewise-linear limit of equation (1) and its one-kink solution (5), (6). To this end, assume that c and s are non-negative, and define the transformation

$$\begin{aligned} &v(x,y) =: \mathrm{e}^{V(x,y)/\varepsilon} \\ &a =: \mathrm{e}^{A/\varepsilon} \qquad f =: \mathrm{e}^{F/\varepsilon} \\ &b =: \mathrm{e}^{B/\varepsilon} \qquad g =: \mathrm{e}^{G/\varepsilon} \\ &c =: \mathrm{e}^{C/\varepsilon} \qquad t =: \mathrm{e}^{T/\varepsilon} \\ &s =: \mathrm{e}^{S/\varepsilon} \end{aligned} \tag{7}$$

where ε is a (small) positive parameter. Using the new variable V and the new parameters, equation (1) becomes

$$\begin{aligned} V(x,y+1) - V(x+1,y) &= \varepsilon \log[1 + \mathrm{e}^{(G+T+V(x,y)-V(x+1,y+1))/\varepsilon}] \\ &\quad - \varepsilon \log[\mathrm{e}^{T/\varepsilon} + \mathrm{e}^{(F+V(x,y)-V(x+1,y+1))/\varepsilon}] \end{aligned} \tag{8}$$

with

$$\mathrm{e}^{F/\varepsilon} + \mathrm{e}^{T/\varepsilon} = 1 + \mathrm{e}^{(G+T)/\varepsilon}. \tag{9}$$

The one-kink solution (5), (6) becomes

$$V(x,y) = \varepsilon \log[1 + \mathrm{e}^{(C+Ax+By+S)/\varepsilon}] - \varepsilon \log[1 + \mathrm{e}^{(C+Ax+By)/\varepsilon}] \tag{10}$$

where

$$\begin{aligned} A &= \varepsilon \log[1 + \mathrm{e}^{(F+S)/\varepsilon}] - \varepsilon \log[\mathrm{e}^{F/\varepsilon} + \mathrm{e}^{S/\varepsilon}] \\ B &= \varepsilon \log[1 + \mathrm{e}^{(G+S)/\varepsilon}] - \varepsilon \log[\mathrm{e}^{G/\varepsilon} + \mathrm{e}^{S/\varepsilon}]. \end{aligned} \tag{11}$$

We can now use the crucial identity [23]

$$\lim_{\varepsilon \downarrow 0} \varepsilon \log[\mathrm{e}^{\alpha/\varepsilon} + \mathrm{e}^{\beta/\varepsilon}] = \max(\alpha, \beta) \tag{12}$$

to obtain the piecewise-linear soliton equation[4]:

$$\begin{aligned} V(x,y+1) - V(x+1,y) &= \max[0, G + T + V(x,y) - V(x+1,y+1)] \\ &\quad - \max[T, F + V(x,y) - V(x+1,y+1)] \end{aligned} \tag{13}$$

where T is (uniquely) determined by[5]

$$\max[F, T] = \max[0, G + T]. \tag{14}$$

(Equations (13) and (14) have been derived under the assumption

$$t = (1-f)(1-g) > 0$$

i.e. $FG > 0$. For $FG < 0$, one obtains a slightly different piecewise-linear soliton equation in which $V(x,y) - V(x+1,y+1)$ is explicitly given in terms of $V(x,y+1) - V(x+1,y)$ with a slightly different definition for T.)

The piecewise-linear one-kink solution becomes

$$V(x,y) = \max[0, Ax + By + C + S] - \max[0, Ax + By + C] \tag{15}$$

with

$$\begin{aligned} A &= \max[0, F + S] - \max[F, S] \\ B &= \max[0, G + S] - \max[G, S]. \end{aligned} \tag{16}$$

[4] Note that equation (13) is invariant under $F \leftrightarrow G$, $x \leftrightarrow y$, $T \leftrightarrow -T$. We therefore restrict our discussion to the case $|G| > |F|$.

[5] If $G \not\equiv 0$.

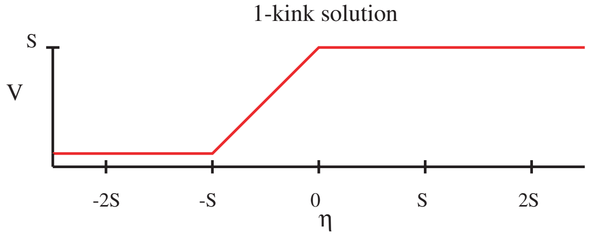

Figure 1. One-soliton solution as a function of the similarity variable $\eta = Ax + By + C$.

A typical kink is plotted in figure 1. Note that the soliton is *completely localized*. This is a crucial feature of piecewise-linear solitons (for other examples of compact solitons see [19]). We can define a 'width':

$$w = \frac{|S|}{\sqrt{A^2 + B^2}} \tag{17}$$

a 'velocity':

$$v = \frac{B}{A} \tag{18}$$

and a height:

$$h = |S|. \tag{19}$$

Plotting A and B as a function of the free parameter S, we obtain (for generic negative values of the parameters F and G) the relationship depicted in figure 2. If $G \neq -\infty$, we may distinguish three regimes:

$$\text{(I)} \quad 0 < |S| < |F| : w = 1/\sqrt{2} \qquad v = 1 \tag{20}$$

$$\text{(II)} \quad |F| < |S| < |G| : w = \frac{|S|}{\sqrt{F^2 + S^2}} \qquad v = \left|\frac{S}{F}\right| \tag{21}$$

$$\text{(III)} \quad |G| < |S| : w = \frac{|S|}{\sqrt{F^2 + G^2}} \qquad v = \frac{G}{F}. \tag{22}$$

Note that in general there is a finite minimum velocity, a finite maximum velocity, and a finite minimum width. The soliton velocity and width as functions of the free parameter S are plotted in figure 3.

2.2. *Piecewise-linear two-kink solution*

Similarly, the two-kink solution of equation (13) is given by

$$\begin{aligned} V(x, y) = \max[&0, A_1x + B_1y + C_1 + S_1, A_2x + B_2y + C_2 + S_2, \\ &(A_1 + A_2)x + (B_1 + B_2)y + C_1 + C_2 + S_1 + S_2 + L] \\ &- \max[0, A_1x + B_1y + C_1, A_2x + B_2y + C_2, \\ &(A_1 + A_2)x + (B_1 + B_2)y + C_1 + C_2 + L] \end{aligned} \tag{23}$$

where

$$\begin{aligned} A_i &:= \max[0, F + S_i] - \max[F, S_i] \\ B_i &:= \max[0, G + S_i] - \max[G, S_i] \end{aligned} \tag{24}$$

and the phase shift L is given by

$$\frac{L}{2} = \max[S_1, S_2] - \max[0, S_1 + S_2]. \tag{25}$$

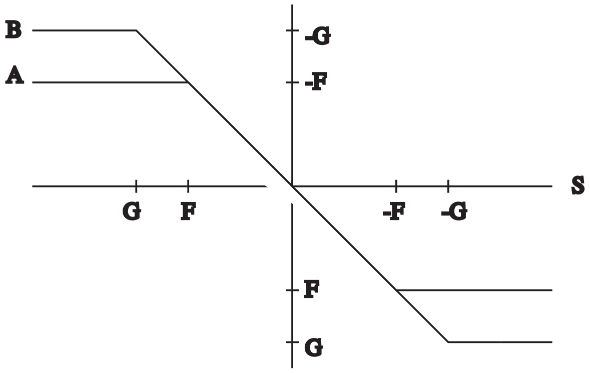

Figure 2. Soliton parameters A and B as a function of S. (For $|S| < -F$, A and B coincide.)

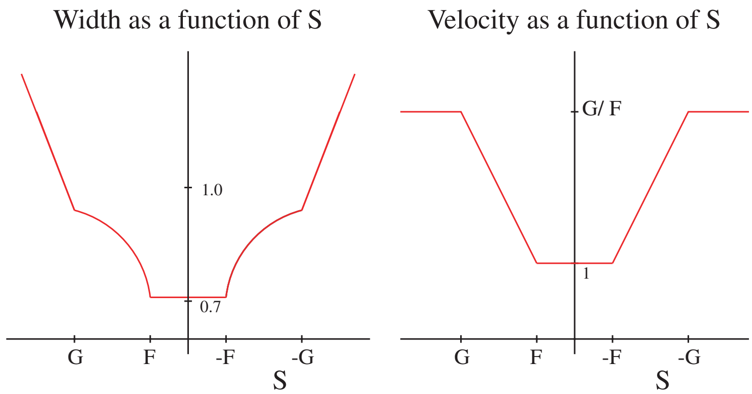

Figure 3. Soliton velocity, v, and width, w, as a function of the free parameter S.

To analyse the general two-kink solution, we introduce

$$\begin{aligned}\eta_1 &= A_1 x + B_1 y + C_1 \\ \eta_2 &= A_2 x + B_2 y + C_2.\end{aligned} \tag{26}$$

Hence the two-kink solution (23) becomes

$$V(\eta_1, \eta_2) = \max[0, \eta_1 + S_1, \eta_2 + S_2, \eta_1 + \eta_2 + S_1 + S_2 + L] - \max[0, \eta_1, \eta_2, \eta_1 + \eta_2 + L]. \tag{27}$$

A schematic plot of $V(\eta_1, \eta_2)$ is given in figure 4 in the case $S_1 < 0$, $S_2 > 0$, $S_1 + S_2 < 0$, $L = 2S_2$ (for other combinations of S_1, S_2 and L, similar pictures can be made). In figure 5 we distinguish nine different regions R1, ..., R9 in which the two-soliton solution is given by

$$\begin{array}{ll} \mathrm{R}1: 0 & \mathrm{R}5: \eta_2 + S_2 \\ \mathrm{R}2: S_1 & \mathrm{R}6: -\eta_1 \\ \mathrm{R}3: S_2 & \mathrm{R}7: -\eta_1 - S_2 \\ \mathrm{R}4: S_1 + S_2 & \mathrm{R}8: \eta_2 + S_1 + 3S_2 \\ & \mathrm{R}9: -\eta_1 - \eta_2 - 2S_2. \end{array} \tag{28}$$

To interpret the soliton behaviour note that in equation (13) $V(x, y+1) - V(x+1, y)$ is explicitly expressed in terms of $V(x, y) - V(x+1, y+1)$. This means that V can be solved

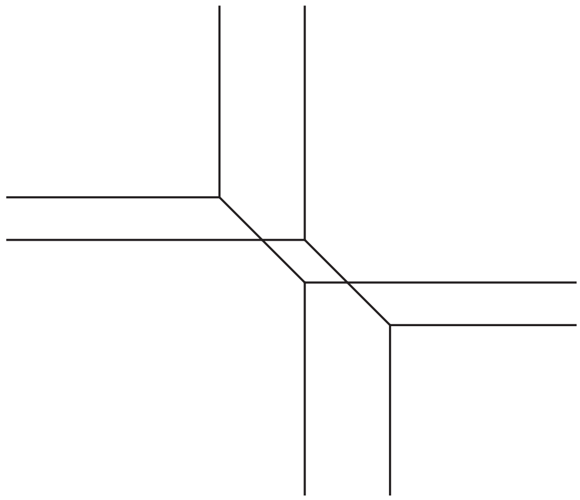

Figure 4. Two-kink solution. The η_1 and η_2 axes are as indicated in figure 5.

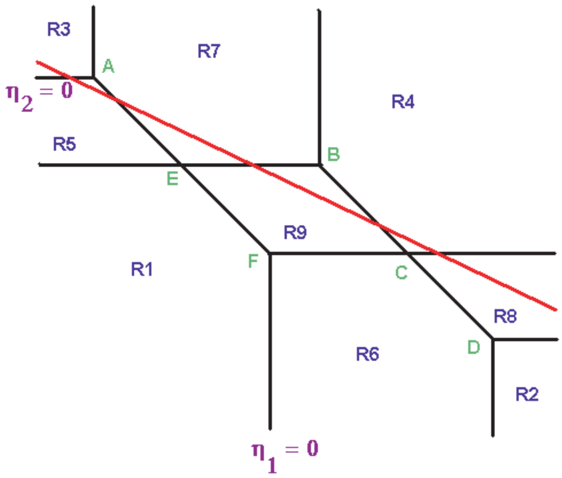

Figure 5. Schematic picture of the regions in the η_1, η_2 plane with different functional forms for the two-kink solution, in the special case $S_1 < 0$, $S_2 > 0$, $S_1 + S_2 < 0$, $L = 2S_2$, with a typical line $\eta_2 = \lambda\eta_1 + \mu$ (as meant in the discussion below equation (30)).

on a lattice $V(x+m, y+n)$, $m, n \in \mathbb{Z}$, specifying initial conditions on the edges of a staircase containing steps to the right in the x direction and upwards in the y direction (and having $V(x, y)$ as one of the edges) as depicted in figure 6.

We now introduce a time variable t and a spatial variable ξ, being a linear combination of x and y such that, on every line of type $\alpha x + \beta y =$ constant, $\alpha\beta > 0$ with only one intersection point with the staircase, t is a monotonically increasing (or decreasing) function of x. This means that we can take $t = (1-\nu)x - \nu y$ with $0 < \nu < 1$ as the time variable. The spatial variable is $\xi = \nu x + (1-\nu)y$. We choose ν such that η_1, the similarity variable of soliton 1, is proportional to ξ, i.e.

$$\nu = \frac{A_1}{A_1 + B_1} \qquad t = \frac{B_1 x - A_1 y}{A_1 + B_1} \qquad \xi = \frac{A_1 x + B_1 y}{A_1 + B_1}. \tag{29}$$

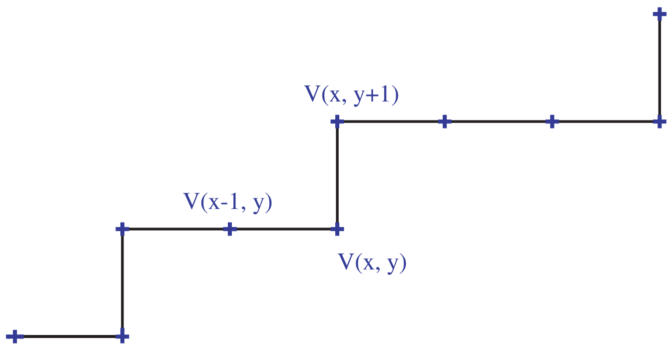

Figure 6. Example of a staircase with edge $V(x, y)$ to specify initial conditions for equation (13).

With (29), η_1 and η_2 can be expressed as

$$\eta_1 = (A_1 + B_1)\xi + C_1 \qquad \eta_2 = \lambda\eta_1 + \mu(t) \tag{30}$$

where

$$\lambda = \frac{A_1A_2 + B_1B_2}{A_1^2 + B_1^2} \qquad \mu(t) = -\frac{t(A_1B_2 - A_2B_1)(A_1 + B_1)}{A_1^2 + B_1^2} + C_2 - C_1\frac{A_1A_2 + B_1B_2}{A_1^2 + B_1^2}.$$

In discussing the qualitative behaviour of the two-soliton solution we consider two cases: (1) $A_1B_2 - A_2B_1 \neq 0$ and (2) $A_1B_2 - A_2B_1 = 0$.

Case 1. $A_1B_2 - A_2B_1 \neq 0$. If the solitons have parameters in different regimes (given by equations (20)–(22)), i.e. (II, I), (III, I), (III, II) or in (II, II) with $S_2 + S_1 < 0$, they have different velocities, i.e. $A_1B_2 - A_2B_1 \neq 0$.

In all cases, we have $-1 < \lambda < S_2/S_1$ and μ is a decreasing function of t. A typical line $\eta_2 = \lambda\eta_1 + \mu$ satisfying this requirement has been drawn in figure 5. By drawing six lines parallel to this line through the points A, B, C, D, E and F we can distinguish seven different regimes (1), (2), (3), (4), (5), (6) and (7) of solitonic behaviour for decreasing t (the line in figure 5 lies in regime (4)).

The two-soliton solution as a function of η_1 in regimes (1), (2), ..., (7) has been sketched in figure 7[6]. A slightly different behaviour in regions (3) and (5) consisting of four lines with slopes $-1, -1-\lambda, -1, \lambda$ and $\lambda, -1, -1-\lambda, -1$, respectively, occurs for λ values closer to -1.

Case 2. $A_1B_2 - A_2B_1 = 0$. Choosing both S_1 and S_2 in regime (I) or in regime (III) we have $A_1B_2 - A_2B_1 = 0$ corresponding to the case that solitons 1 and 2 have the same velocity. In that case we have a 'stationary solution' not depending on t and being only a function of the variable ξ. The values of λ in (I, I) and (III, III) are S_2/S_1 and -1, respectively, and are limiting cases of the λ values in case 1.

In regime (I, I), depending on C_1 and C_2, we can have stationary solutions with η_1 dependence as in regimes (1), (3), (5) and (7) of figure 5. In regime (III, III) with $\lambda = -1$ we only have stationary solutions with η_1 as in regimes (1) and (7). In the limiting case $S_2 = -S_1$ we can also have stationary solutions with solitons 1 and 2 in regime (II), the slope λ in that case being equal to -1.

[6] The situation sketched in figure 7 corresponds to the case $\frac{2S_2}{S_1-S_2} < \lambda < S_2/S_1$. A similar picture can be found in the case when $-1 < \lambda < \frac{2S_2}{S_1-S_2}$.

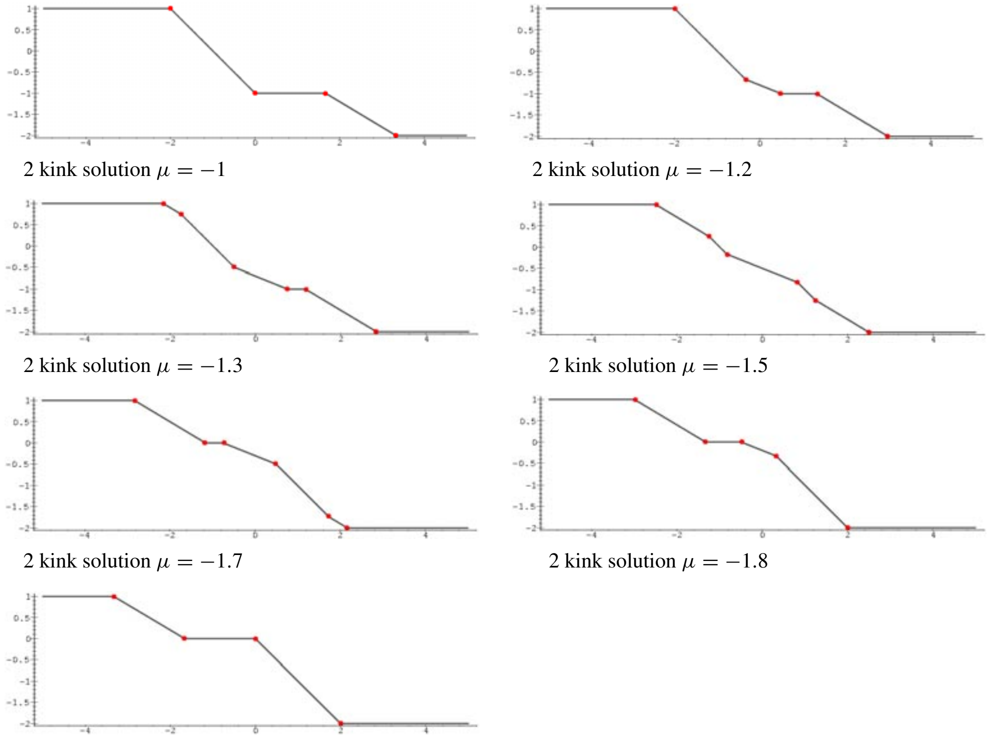

2 kink solution $\mu = -1$ 2 kink solution $\mu = -1.2$

2 kink solution $\mu = -1.3$ 2 kink solution $\mu = -1.5$

2 kink solution $\mu = -1.7$ 2 kink solution $\mu = -1.8$

2 kink solution $\mu = -2$

Figure 7. The seven stages of the two-kink collision for the case $\frac{2S_2}{S_1-S_2} < \lambda < \frac{S_2}{S_1}$. The two-kink solution V as a function of η_1 is plotted for different values of μ and for a generic choice of the parameters ($S_1 = -2$, $S_2 = 1$, $\lambda = -0.6$). The large kink is coming in from the left and coming out at the right. The small kink is the opposite of this.

2.3. Piecewise-linear Lax representation

We also derive a Lax representation for the piecewise-linear equation (13). The summation and multiplication of two matrices A and B in the piecewise-linear version are defined by

$$\begin{aligned} [A \oplus B]_{ij} &:= \max(A_{ij}, B_{ij}) \\ [A \otimes B]_{ij} &:= \max_k (A_{ik} + B_{kj}). \end{aligned} \tag{31}$$

Similarly, the 'Trace' of a matrix A, and the inner product with a vector $\underline{a}$, are given by

$$\begin{aligned} \mathrm{Tr}\, A &= \max_k A_{kk} \\ [A \otimes a]_i &= \max_k (A_{ik} + a_k). \end{aligned} \tag{32}$$

The Lax representation (3), (4) thus becomes

$$\underline{U}(x+1, y) = \underline{\underline{L}}(x, y) \otimes \underline{U}(x, y) \qquad \underline{U}(x, y+1) = \underline{\underline{M}}(x, y) \otimes \underline{U}(x, y) \tag{33}$$

with

$$\begin{aligned} \underline{\underline{L}}(x, y) &= \begin{pmatrix} F & T + V(x+1, y) \\ T + K - V(x, y) & V(x+1, y) - V(x, y) \end{pmatrix} \\ \underline{\underline{M}}(x, y) &= \begin{pmatrix} G & V(x, y+1) \\ K - V(x, y) & V(x, y+1) - V(x, y) \end{pmatrix}. \end{aligned} \tag{34}$$

The 'Trace' of a matrix product is invariant under cyclic shifts:

$$\mathrm{Tr}\, A \otimes B = \sum_{i,k} \max(A_{ik} + B_{ki}) = \mathrm{Tr}\, B \otimes A. \tag{35}$$

The compatibility condition of (33) and (34), i.e.

$$L(x, y+1) \otimes M(x, y) = M(x+1, y) \otimes L(x, y) \tag{36}$$

leads to the piecewise-linear soliton equation (13), as can be seen as follows: substituting (34) into (36), and using (31), one finds that the (1, 1) elements on the right- and the left-hand sides of (36) are identical, as are the (2, 2) elements. The (1, 2) and (2, 1) elements yield

$$\begin{aligned}&\max[F + V(x, y+1), T + V(x+1, y+1) + V(x, y+1) - V(x, y)]\\ &\quad = \max[G + T + V(x+1, y), V(x+1, y+1) + V(x+1, y) - V(x, y)]\end{aligned} \tag{37}$$

and

$$\begin{aligned}&\max[T + G + K - V(x, y+1), K + V(x+1, y+1) - V(x, y+1) - V(x, y)]\\ &\quad = \max[F + K - V(x+1, y), T + K + V(x+1, y+1)\\ &\qquad - V(x+1, y) - V(x, y)]\end{aligned} \tag{38}$$

respectively. It is now easy to see that the dependence of the spectral parameter K drops out of equation (38), and that both (37) and (38) are equivalent to the piecewise-linear soliton equation (13). (The above derivation applies in the case $FG > 0$. In the other case, $FG < 0$, a slightly different Lax representation has to be used in order to find the piecewise-linear equation with $V(x, y) - V(x+1, y+1)$ explicitly given in terms of $V(x, y+1) - V(x+1, y)$.)

Finally, note that the Lax representation (33) is linear in $\underline{U}(x, y)$ with respect to the max operation. That is, if $U_1(x, y)$ and $U_2(x, y)$ are solutions of (33), so is $\underline{\tilde{U}}$ with components $\tilde{U}_i = \max[\lambda + U_{1i}, \mu + U_{2i}]$.

3. Piecewise-linear lump solitons

Defining

$$W(x, y) := V(x, y) - V(x+1, y+1) \tag{39}$$

it follows that W satisfies the following equation:

$$\begin{aligned}W(x, y+1) - W(x+1, y) &= \max[0, G + T + W(x, y)]\\ &\quad - \max[T, F + W(x, y)] - \max[0, G + T + W(x+1, y+1)]\\ &\quad + \max[T, F + W(x+1, y+1)]\end{aligned} \tag{40}$$

and the lump solitons follow by inserting (15) and (23) in (39). A typical lump soliton is given in figure 8. Note that it is completely localized.

4. Piecewise-linear integrable maps

One can also derive piecewise-linear integrable maps from smooth integrable maps, using a transformation similar to the one given in (7). For example, from an eight-parameter subset of the 18-parameter family of integrable maps of the plane given in [17], one obtains the following piecewise-linear integrable map [21]:

$$\begin{aligned}X' &= -X + \max(F + Y, H, J - Y) - \max(A + Y, B, E - Y)\\ Y' &= -Y + \max(E + X', G, J - X') - \max(A + X', C, F - X')\end{aligned} \tag{41}$$

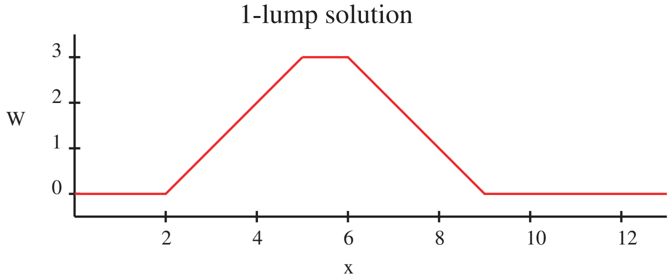

Figure 8. A one-lump soliton obtained by substituting the parameter values $A = -2$, $B = -1$, $C = 5$, $F = -1$, $G = -1$ and $S = 4$ at $y = 0$ into equation (15) and in turn substituting this expression into equation (39).

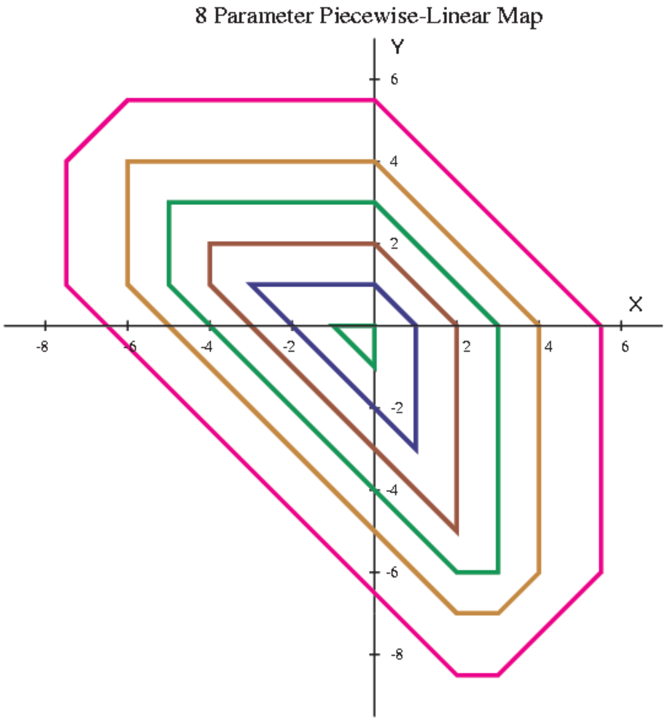

Figure 9. A plot of the eight-parameter piecewise-linear integrable map, where the parameters A, B, C, E, F, G, H and J are equal to 2, 2, 2, −4, −4, −1, 0 and 1, respectively. The number of sides possessed by each invariant polygon decreases from 8 to 7 to 6 to 5 to 4 and then to 3.

where A, B, C, E, F, G, H, J are arbitrary parameters in $\mathbb{R} \cup -\infty$.

The map (41) is area-preserving, reversible, and possesses the piecewise-linear integral

$$I(X,Y) = \max(A + X + Y, B + X, C + Y, E + X - Y, F - X + Y, G - Y, H - X, J - X - Y). \tag{42}$$

A phase plot for the map (41) is given in figure 9.

Figure 10. Staircase and mapping in the special case $z_1 = z$, $z_2 = 1$.

In the special case of $X - Y$ symmetry, (41) and (42) can be reduced to

$$\begin{aligned} X' &= -Y + \max(C + X, E, F - X) - \max(A + X, B, C - X) \\ Y' &= X \end{aligned} \tag{43}$$

and

$$\begin{aligned} I(X, Y) = \max(&A + X + Y, B + X, B + Y, C + X - Y, C - X + Y, \\ &E - Y, E - X, F - X - Y). \end{aligned} \tag{44}$$

More details of the maps (41) and (43) will be given in a separate paper.

One can also derive piecewise-linear integrable maps from equation (13). To this end, consider solutions of equation (13) that satisfy a periodicity property

$$V(x, y) = V(x + z_1, y + z_2). \tag{45}$$

If this is the case, we can specify initial conditions on a staircase connecting (x, y) and $(x + z_1, y + z_2)$ by z_1 horizontal steps to the right and z_2 upward vertical steps. Defining a mapping by a horizontal shift

$$V(x, y) \longrightarrow V'(x, y) = V(x + 1, y)$$

we obtain a $(z_1 + z_2)$-dimensional mapping for the fields V_k at the vertices of the staircase and their iterates (where $k = z_2 x - z_1 y$).

As an example, we consider here the special case $z_1 = z$, $z_2 = 1$ (sketched in figure 10). We obtain the $(z + 1)$-dimensional mapping

$$\begin{aligned} V_0' &= V_1 \\ V_1' &= V_2 \\ \vdots\ & \quad \vdots \\ V_{z-1}' &= V_z \\ V_z' &= V_0 + \max[0, G + T + V_z - V_1] - \max[T, F + V_z - V_1]. \end{aligned} \tag{46}$$

(Note that, defining $Z_i := V_{i+1} - V_i$, equation (46) reduces to a z-dimensional mapping.)

To find the integrals, consider the monodromy matrix along the staircase

$$\tau = M(x + z, y) \otimes L(x + z - 1, y) \otimes \cdots \otimes L(x + 1, y) \otimes L(x, y) \tag{47}$$

with M and L given by equation (34).

The monodromy matrix after a horizontal shift is given by τ', which is obtained from τ, replacing the V_k by the iterated quantities V_k'.

From the compatibility condition and the periodicity (45), we find

$$\tau' = L(x, y) \otimes M(x + z, y) \otimes L(x + z - 1, y) \otimes \cdots \otimes L(x + 1, y) \tag{48}$$

and using the invariance of the 'Trace' as in equation (35) we have

$$\mathrm{Tr}(\tau') = \mathrm{Tr}(\tau) \tag{49}$$

implying that also in the piecewise-linear case the integrals of the mapping are given by the 'Trace' of the monodromy matrix, defined by (32) and (47).

The actual evaluation of the invariants for general z is similar to the analytic case in [15]. For $z = 2$ we have, taking $V_1 - V_0 = Z_0$ and $V_2 - V_1 = Z_1$,

$$I = \max[2F + G - K - T, G + T + Z_0 + Z_1, F - Z_0, Z_1, F - Z_1, \\ Z_0, T - Z_0 - Z_1, -K - T]. \qquad (50)$$

Here K is a spectral parameter which may have arbitrary values. Taking $K \to \infty$, both K-dependent terms do not contribute to the maximum and can be dropped.

Proceeding in a similar way for $z = 3$ and removing (constant) K-dependent terms, we obtain the integral, taking $V_2 - V_0 = U_0$ and $V_3 - V_1 = U_1$,

$$I = \max[T + F + G + U_0, 2F - U_0, F + G + T + U_1, G + T + U_0 + U_1, F - U_0 + U_1, U_1, \\ 2F - U_1, F + U_0 - U_1, F + T - U_0 - U_1, T - U_1, U_0, T - U_0]. \qquad (51)$$

The piecewise-linear mappings for $z = 2$ and 3 with integrals I given by (50) and (51) are special cases of equation (43). (Another special case was treated in [22].)

In case $z \geqslant 4$, different K-dependent terms under the maximum contain nontrivial contributions in terms of the fields $V_0, \ldots, V_z$, yielding two or more integrals of the mappings.

5. Concluding remarks

5.1. Differences between ultradiscrete and piecewise-linear systems

In the introduction we noted that an important difference between ultradiscrete and piecewise-linear systems (as defined there) is that in the former the variables and parameters are restricted to be integers, whereas in the latter they are real numbers. This fact (and specifically the many degenerate maxima in the ultradiscrete case) makes the analysis of piecewise-linear systems much more straightforward. (The results concerning ultradiscrete systems may be inferred as special cases.) Consider, for example, figure 9. If we restricted the values of the variables X and Y to be integers, the analysis (as given in [21]) of changes occurring in the shapes of the invariant sets would become much more complicated. Similarly, the analysis of bifurcations associated with continuous parameter changes would become impossible. Similar comments can be made concerning the analysis of two-kink solutions, etc.

5.2. Physical relevance

As mentioned above, a general aspect of piecewise-linear solitons is that they are compact (liberating us from 'the infinite tail of solitons one learns to live with but (that) should not be mistaken for reality' [20]). One could argue that limits such as (7), and hence non-analytic equations such as (13), do not occur in physics as such, but we expect the piecewise-linear equations to give qualitative insight concerning the various stages of soliton-scattering processes. Furthermore it should be realized that, for small but finite ε, the analytic equation (8) and its analytic solutions are extremely similar to equation (13) and its solutions.

As far as our specific model (13) goes, one of the important physical aspects of its kink solutions is the existence of a minimum and maximum velocity, and a minimum width (see figure 3). In the limit as $G \to -\infty$, the maximum velocity goes to ∞, and the model exhibits tachyon-like particles with minimum velocity 1. It would be interesting to see if other piecewise-linear soliton equations exhibit similar properties. This may be addressed following the lines of this paper starting from other known integrable difference equations in two [11, 16] and three dimensions [10, 12].

Acknowledgments

We are grateful to the Australian Research Council, the Stichting voor Fundamenteel Onderzoek der Materie (FOM), the Nederlandse Organisatie voor Wetenschappelijk Onderzoek (NWO), and the EPSRC for financial support.

References

[1] Ablowitz M J and Clarkson P 1991 *Solitons, Nonlinear Evolution Equations and Inverse Scattering* (Cambridge: Cambridge University Press)
[2] Ablowitz M J and Ladik J F 1977 On the solution of a class of nonlinear partial difference equations *Stud. Appl. Math.* **57** 11–2
[3] Arnol'd V I 1989 *Mathematical Methods of Classical Mechanics* (Berlin: Springer)
[4] Audin M 1996 *Spinning Tops* (Cambridge: Cambridge University Press)
[5] Bruschi M, Ragnisco O, Santini P M and Tu Gui-Zhang 1991 Integrable symplectic maps *Physica* D **49** 273–94
[6] Calogero F and Degasperis A 1982 *Spectral Transform and Solitons* (Amsterdam: North-Holland)
[7] Grammaticos B, Nijhoff F W and Ramani A 1999 Discrete Painlevé equations *The Painlevé Property, One Century Later* ed R Conte (Berlin: Springer) pp 417-552
[8] Hirota R, Iwao M, Ramani A, Takahashi D, Grammaticos B and Ohta Y 1997 From integrability to chaos in a Lotka–Volterra cellular automaton *Phys. Lett.* A **236** 39–44
[9] Hirota R and Tsujimoto S 1995 Conserved quantities of a class of nonlinear difference-difference equations *J. Phys. Soc. Japan* **64** 3125–7
[10] Nijhoff F W and Capel H W 1990 The direct linearisation approach to hierarchies of integrable PDEs in 2 + 1 dimensions: I. Lattice equations and the differential-difference hierarchies *Inverse Problems* **6** 567–90
[11] Nijhoff F W and Capel H W 1995 The discrete Korteweg–de Vries equation *Acta Appl. Math.* **39** 133–58
[12] Nijhoff F W, Capel H W, Wiersma G L and Quispel G R W 1984 Bäcklund transformations and three-dimensional lattice equations *Phys. Lett.* A **105** 267–72
[13] Papageorgiou V G, Nijhoff F W and Capel H W 1990 Integrable mappings and nonlinear integrable lattice equations *Phys. Lett.* A **147** 106–14
[14] Park K, Steiglitz K and Thurston W P 1986 Soliton-like behaviour in automata *Physica* D **19** 423–32
[15] Quispel G R W, Capel H W, Papageorgiou V G and Nijhoff F W 1991 Integrable mappings derived from soliton equations *Physica* A **173** 243–66
[16] Quispel G R W, Nijhoff F W, Capel H W and van der Linden J 1984 Linear integral equations and nonlinear difference-difference equations *Physica* A **125** 344–80
[17] Quispel G R W, Roberts J A G and Thompson C J 1988 Integrable mappings and soliton equations I *Phys. Lett.* A **126** 419–21
[18] Quispel G R W, Roberts J A G and Thompson C J 1989 Integrable mappings and soliton equations II *Physica* D **34** 183–92
[19] Rosenau P 1996 On solitons, compactons, and Lagrange maps *Phys. Lett.* A **211** 265–75
[20] Rosenau P 1997 On nonanalytic solitary waves formed by a nonlinear dispersion *Phys. Lett.* A **230** 305–18
[21] Scully J 1999 An exploration of integrable two-dimensional maps *Honours Thesis* Mathematics Department, La Trobe University
[22] Takahashi D, Tokihiro T, Grammaticos B, Ohta Y and Ramani A 1997 Constructing solutions to the ultradiscrete Painlevé equations *J. Phys. A: Math. Gen.* **30** 7953–66
[23] Tokihiro T, Takahashi D, Matsukidaira J and Satsuma J 1996 From soliton equations to integrable cellular automata through a limiting procedure *Phys. Rev. Lett.* **76** 3247–50
[24] Veselov A P 1991 Integrable mappings *Russ. Math. Surv.* **46** 1–51